Applications of ICFD solver by LS-DYNA® in Automotive Fields to Solve Fluid-Solid-Interaction (FSI) Problems

George Wang(1*), Facundo del Pin(2), Inaki Caldichoury (2), Prince Rodriguez(3), Jason Tippie (3), Shane Smith (3)

(1) Vehicle Structure – Automotive Safety, (3) Power Sports Products
21001 State Route 739, Raymond, OH 43067-9705
(2) Livermore Software Technology Corporation
7374 Las Positas Road, Livermore, CA, 94551

*Corresponding author: gwang@oh.hra.com

Key words: fluid-structure interaction, ICFD, gear box flow, thermal muffler flow, windshield buffeting

Abstract

Fluid-solid interaction (FSI) becomes a more and more important and wider application field in the automotive industry. It is challenging to CAE engineers to predict performance of complicated systems under high speed flow and with dynamic free surface evolution. This paper presents the three following FSI accomplishments in the power sports field by using ICFD solver from LS-DYNA®:

(1) Gear box oil flow driven by high spinning speed shafts. The goal of this work was to develop a CAE method to predict if oil in the gear box leaks out of the fuel hole at three gear box positions ($0^0, 15^0, 40^0$) and two rotation speeds (1060 and 3320 rpm). The CAE results completely comply with the test data.
(2) Thermal flow in muffler. This CAE work was to investigate how the exhaust heat flow from the engine causes a temperature transfer along the muffler surface. Anisotropic porous modeling is used to model the flow through the catalytic converter and the CAE results are validated, respectively, by (i) the test flow rate data under constant temperature and (ii) the exhaust conjugate heat transfer test data. The results show good correlation.
(3) Windshield buffeting. This project was done to explore if the window and roof of a side-by-side MUV would fail by wind force.

Introduction

Due to the dramatic development of computer technology and engineering software, it becomes possible to solve complex fluid solid interaction (FSI) problems in modern automotive fields. In

modern vehicle design, gear box oil flow, thermal flow in muffler and vehicle structure buffeting, etc., are the some of the highly concerning areas that make challenging FSI problems.

FSI in meaning is a coupling process between flow and solid in time and it occurs whenever the flow effect on the structure causes it deformation and even failure and the deformed structure interacts with the flow field. To predict these interactions, a highly sophisticated software is required to be able to simulate the fluid and the structural part evolving into a dynamic coupled system in which the fluid forces applied to the solid causes the solid to displace at each time step.

LS-DYNA® Version R8.1 includes the incompressible flow solver (ICFD) which can solve FSI problems [1]. It uses an implicit solver to solve the strong FSI process listed in Figure 1 [2]. Recently the LS-DYNA ICFD solver was used to solve many FSI problems with good success [3-7].

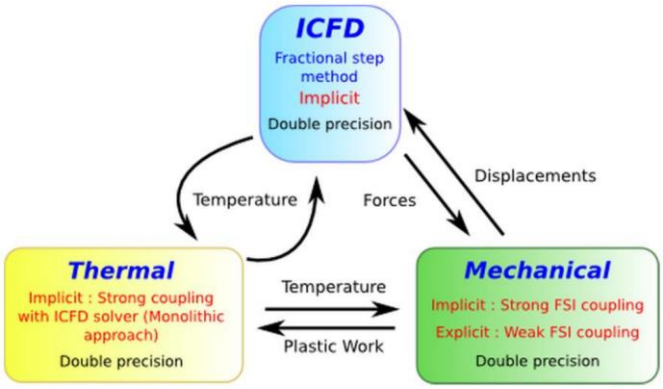

Figure 1 FSI solver process in LS-DYNA®ICFD

Next, we present three FSI accomplishments in Honda R&D, Ohio. LS-DYNA® Version 8.1 is applied.

FSI Applications at Honda R&D, Ohio

1. Gear box oil flow

The objective of this work is to help designers to judge if the lubricating oil in a transmission box leaks out of the fuel hole at some critical positions and gear rotational speeds to help improve the design when a problem occurs.

Figure 2 shows the three experiments at Honda Power Sports Division at Ohio. Three gear box positions were tested at $0^0, 15^0$ and 40^0, and combined with the two rotation speeds of 1056 rpm and 3320 rpm, respectively. Among all of the three tests, no oil leak is observed out of the fuel hole in Tests (a) and (c) while oil leak seen in Test (b).

The oil parameters are: density=0.904 g/cm^3 and dynamic viscosity = 384 $mpa \cdot s$. In the simulations, the gears and gearbox surfaces are set as rigid. The one-way coupling parameter OWC =1 is used in *ICFD_CONTROL_FSI.

(a) $0^0, 3320\ rpm$ (b) $15^0, 3320\ rpm$ (c) $40^0, 1056\ rpm$

Figure2 Experiments of gear box oil flow

1.1 Model setup

Figure 3 shows the exact oil level in the box for Tests (a-c). Figure 4 (a-b) shows the assembled ICFD fluid surface mesh and solid element mesh in the CAE model. Pid =4 describes the fuel hole area to calculate flux to judge oil leakage. Pid=5 is the fluid surface. Note that since the current ICFD solver cannot solve the moving fluid boundary mesh, moving gear shafts are set with a small gap of ~ 1 mm to the gearbox boundary as seen in Figure 5. A non-slip condition is set to the fluid boundary. LES is selected as the turbulence model.

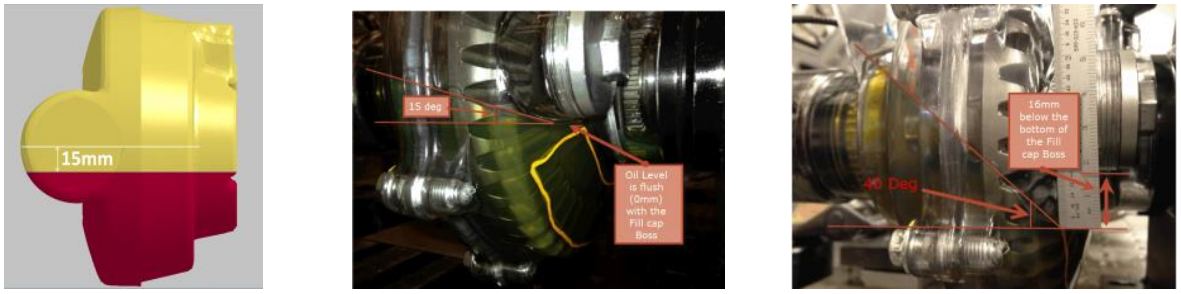

Test (a) Test (b) Test (c)

Figure 3 Oil level in Tests (a-c)

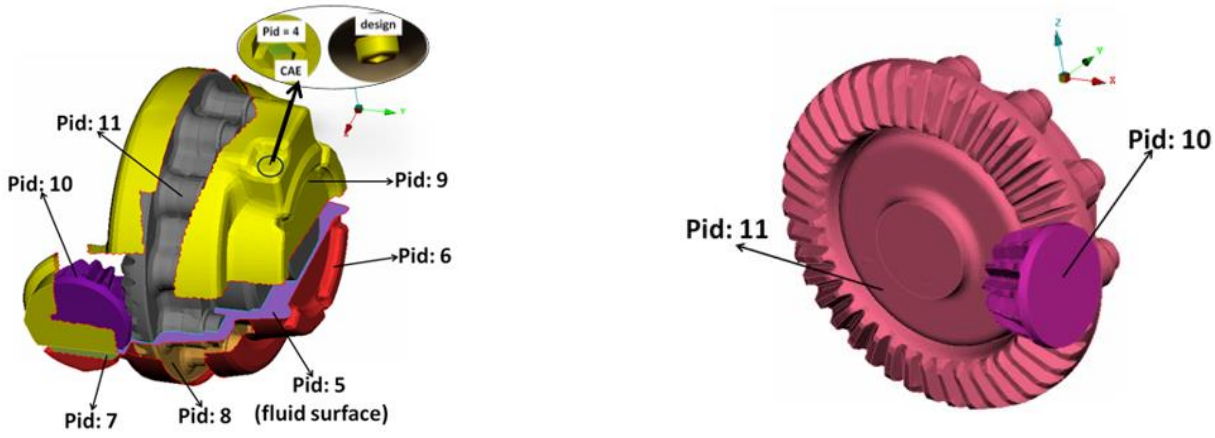

(a) ICFD fluid surface mesh (b) Solid element mesh

Figure 4 Assembled CAE mesh for gearbox

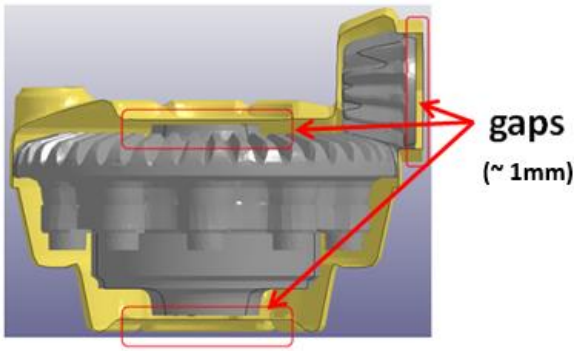

Figure 5 Gears in the box

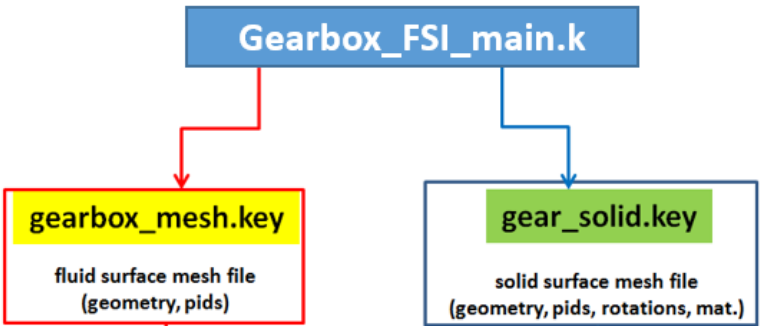

Figure 6 FSI process of gear box flow simulation

Figure 6 shows the link between the fluid surface mesh and the solid geometry mesh of the gears.

1.2 Results

1.2.1 CAE vs test (a)

The following figures show the results of the CAE compared to the test. Since the net flux value is zero, no oil leak is predicted. This matches the observation in the test.

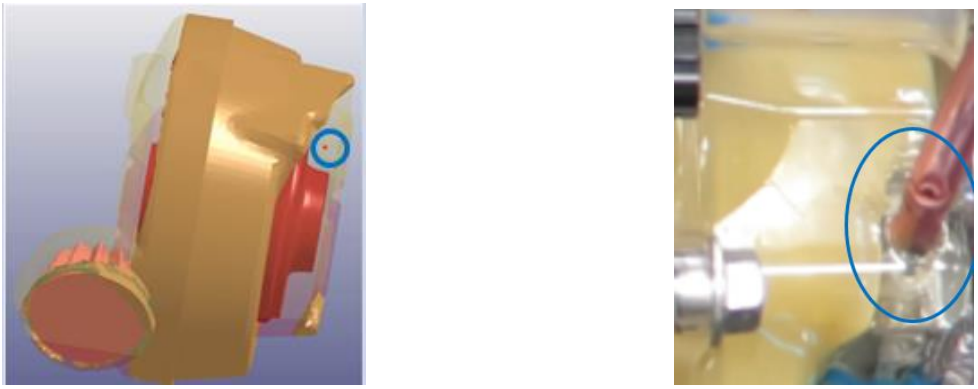

(a) CAE result (b) Experiment

Figure 7 Comparison between the CAE and test with flow level at stabilized stage

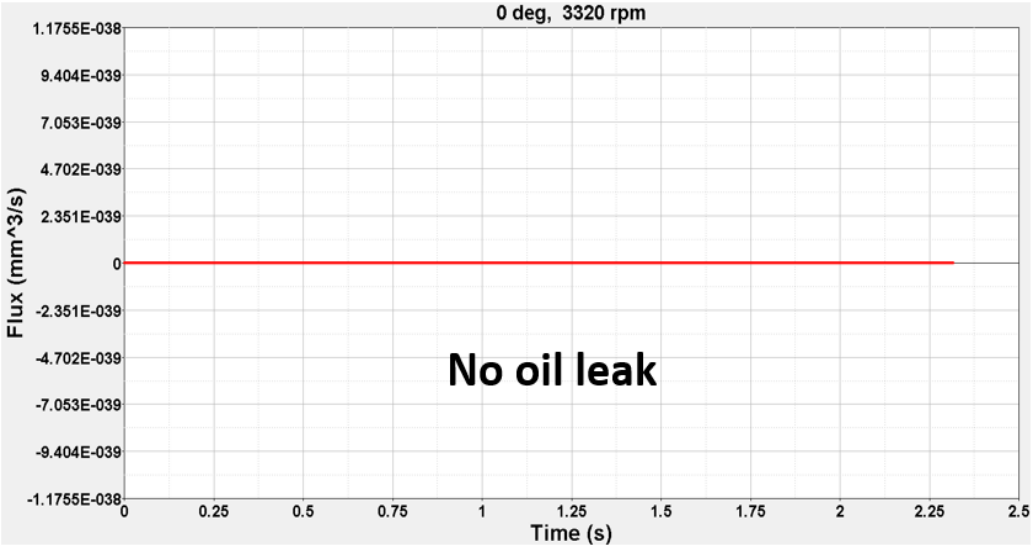

Figure 8 Flux at the fuel hole from the CAE model

1.2.2 CAE vs test (b)

The following figures show the CAE and test results for test (b) where an oil leak occurred. Figure 10 shows the net flux as non-zero later in the simulation indicating an oil leak.

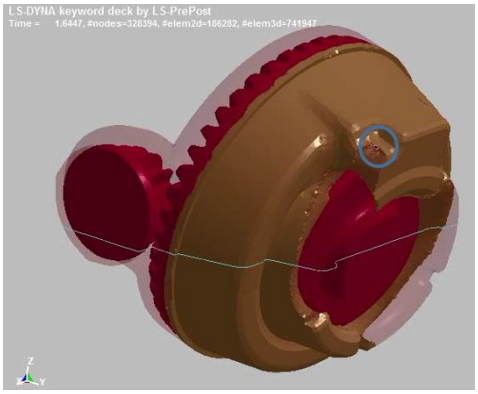

(a) CAE result (b) Experiment

Figure 9 Comparison between the CAE and test with flow level at stabilized stage

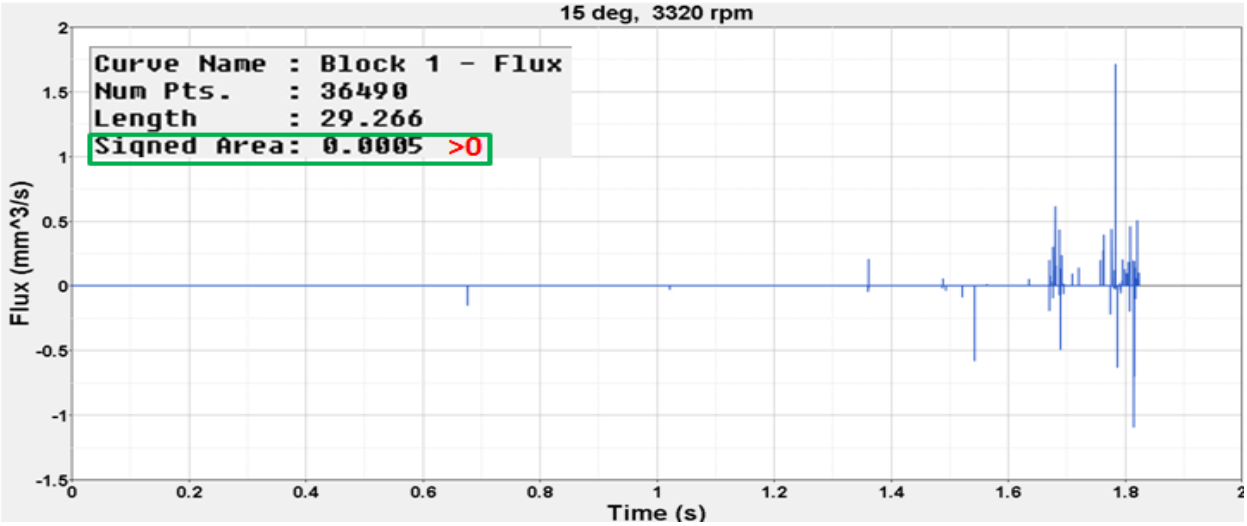

Figure 10 Flux at the fuel hole from the CAE model

1.2.3 CAE vs test (c)

The next set of figures show the results for Test (c) which also showed no oil leak. The zero net flux from the CAE confirms that prediction.

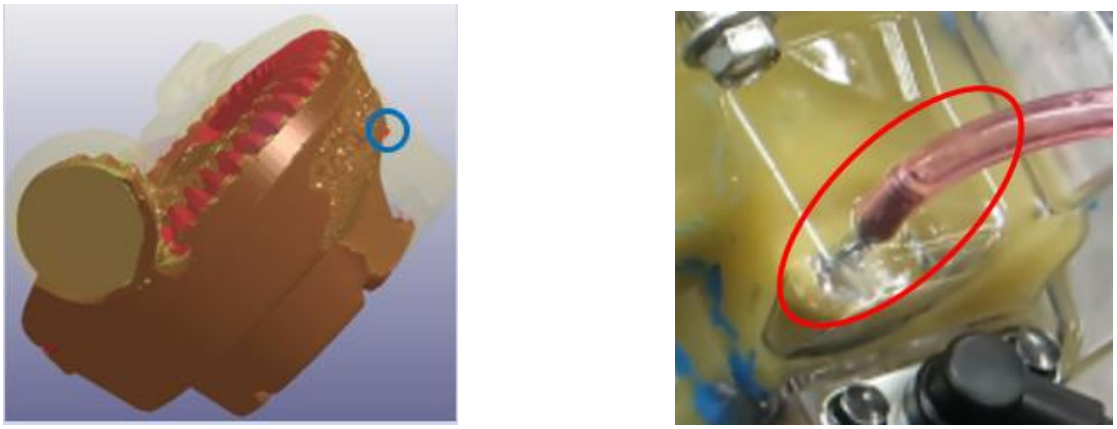

(a) CAE result (b) Experiment

Figure 11 Comparison between the CAE and test with flow level at stabilized stage

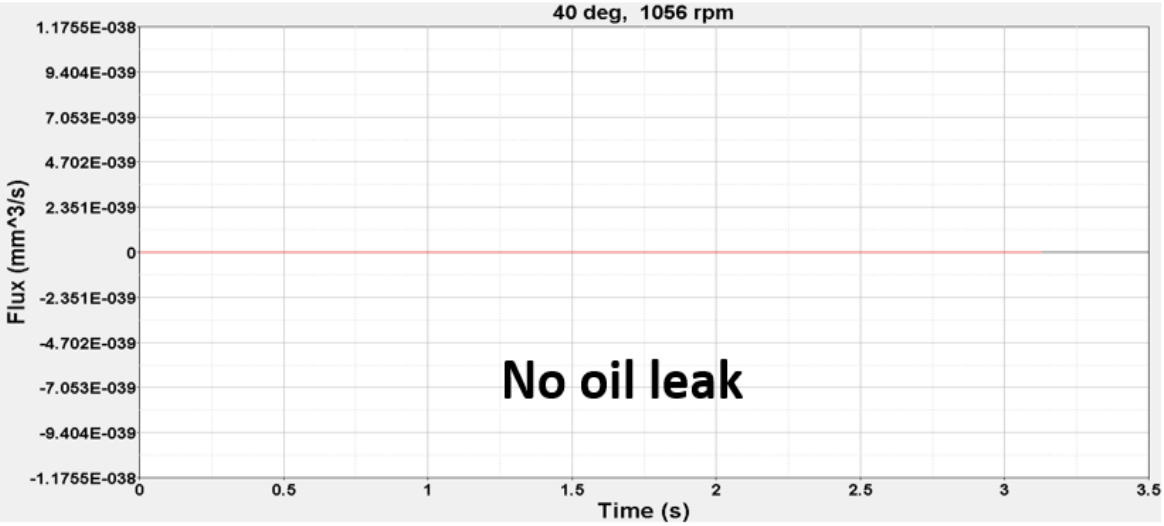

Figure 12 Flux at the fuel hole from the CAE model

2. Conjugate Heat Transfer in Muffler

The next type of analysis is using conjugate heat transfer to help reach a qualified muffler design. Two muffler flow tests were conducted at Power Sports Division, Honda R&D Americas, Inc., Ohio, USA. The CAE predictions vs experiment comparisons are discussed below.

2.1 Constant Temperature Flow in Muffler

Figure 13 (a-b) illustrates the test layout. Air was pumped into the muffler inlet at three pressure values: 300, 200 and 100 mmH_2O and the three corresponding flow rates were measured as seen in Figure 14. Based on the diameter of the pipe (D=54.8 mm) the measured velocity values are 18.19, 14.57 and 9.77 m/s based on the input pressures given above.

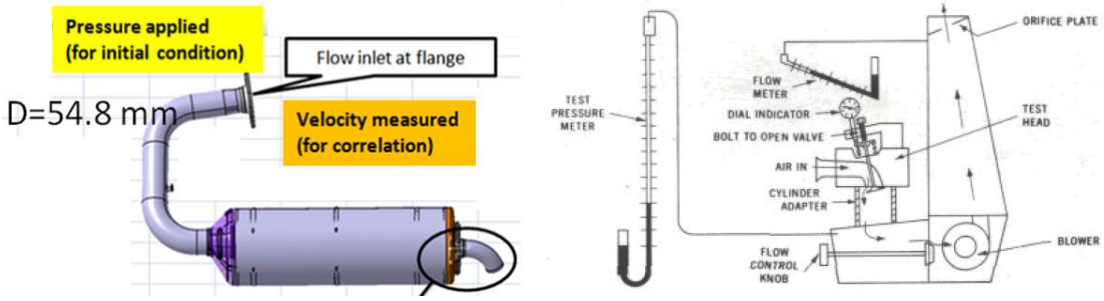

(a) Muffler structure (b) Test equipment layout

Figure 13 Experiment layout for constant temperature flow test

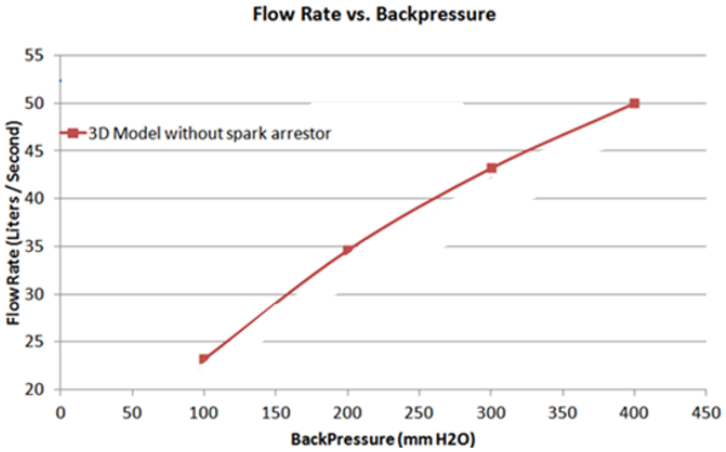

Figure 14 Experiment measurement

2.1.1 Model setup

Figure 15 shows the assembled ICFD fluid surface mesh. A non-slip condition was again applied to the fluid boundary and LES is selected for the turbulence model. The muffler surfaces were defined as a rigid material. Air density and dynamic viscosity are set at 1.292 kg/m^3 and $1.86 \times 10^{-5} kg/m\ s$. An anisotropic porous model is included in LS-DYNA® Version 8.1 to solve the flow through a catalytic converter. The following model parameters are defined by using the test data: porosity $\varepsilon = 0.96$, permeability $\kappa = 4.55 \times 10^{-5} m^2$, and Forchheimer factor $F = 0$.

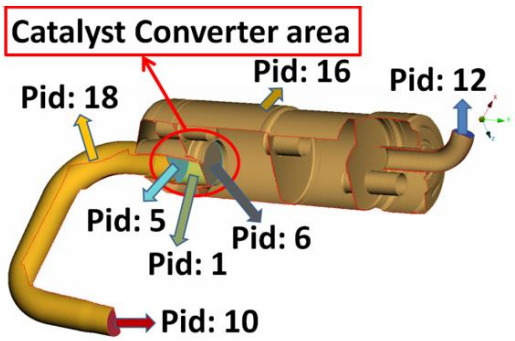

Figure 15 Assembled ICFD surface mesh of muffler

2.1.2 Results

Table 1 shows the comparison between the CAE results of velocity with the values measured in the test. The CAE results are within the targeted accuracy range.

Test No.	Pressure Drop at inlet (Pa)	Velocity at inlet (m/s)	
		Test	CAE
1	2492	18.19	15.03 (-17.4%)
2	1961	14.57	12.27 (-15.8%)
3	981	9.77	8.7 (-10.9%)

Table 1 Comparison between the CAE and test results

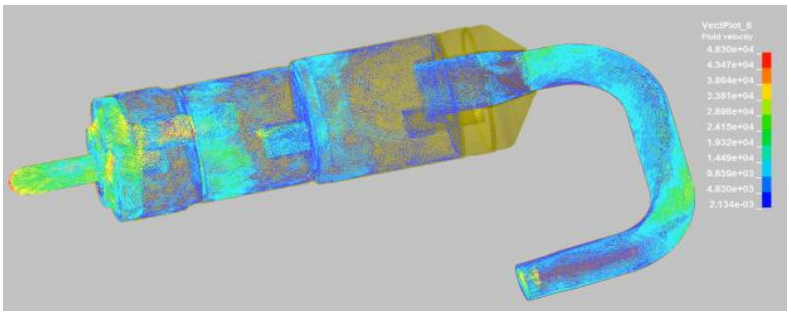

(a) Test 1

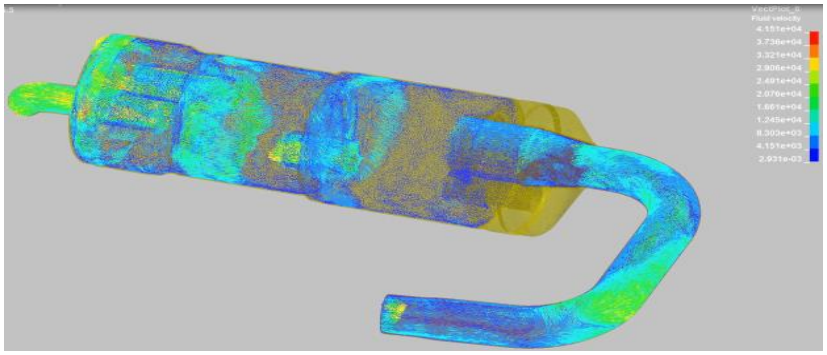

(b) Test2

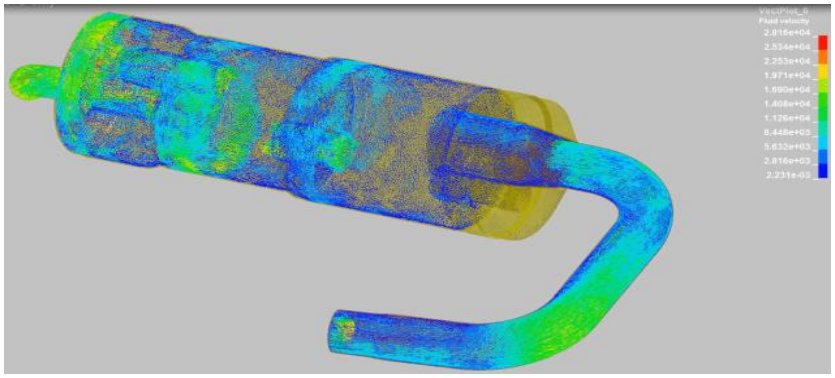

(c) Test 3

Figure 16 CAE predicted stabilized flow fields

2.2 Conjugate heat transfer in Muffler

The following figure illustrates the conjugate heat transfer test layout. For the muffler structure illustrated in Figure 17 (a), the mean air pressure values from the engine were measured at the inlets of the two pipes (rear and front). In Figure 17 (b) the measured mean pressure at the collector location is shown which is used to compare with the CAE result.

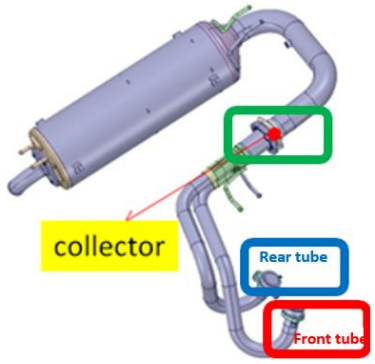

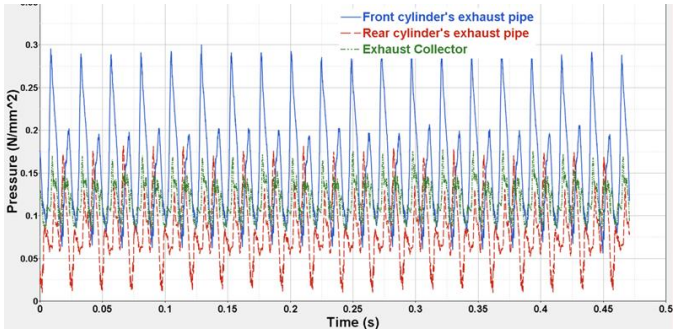

(a) Muffler structure (b) Mean pressure measurement

Figure 17 conjugate heat transfer test layout

2.2.1 Model setup

Figure 18 (a-b) shows the assembled ICFD surface mesh and solid element mesh in the CAE model. Figure 19 shows the FSI process.

The steel muffler is set as rigid and its thermal parameters (conductivity, specific heat, convection heat transfer coefficient, radiation heat transfer coefficient, etc.) were set based on published standards and are not listed here.

The initial temperature for the two inlet pipes (pid=10 and 11) and outlet (pid=12) in Figure 18 (a) are 550℃, 574℃ and 543℃ respectively. A non-slip condition was given to the fluid boundary and LES was selected for the turbulence model.

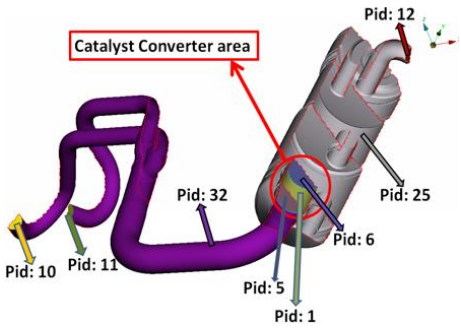

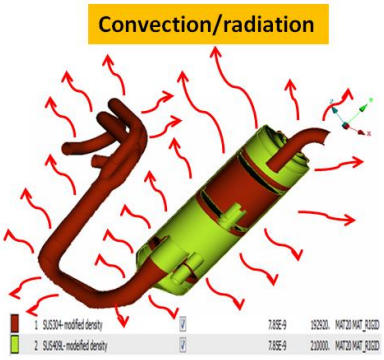

(a) ICFD fluid surface mesh (b) solid element mesh

Figure 18 Assembled mesh for heat conjugate muffler flow in the CAE model

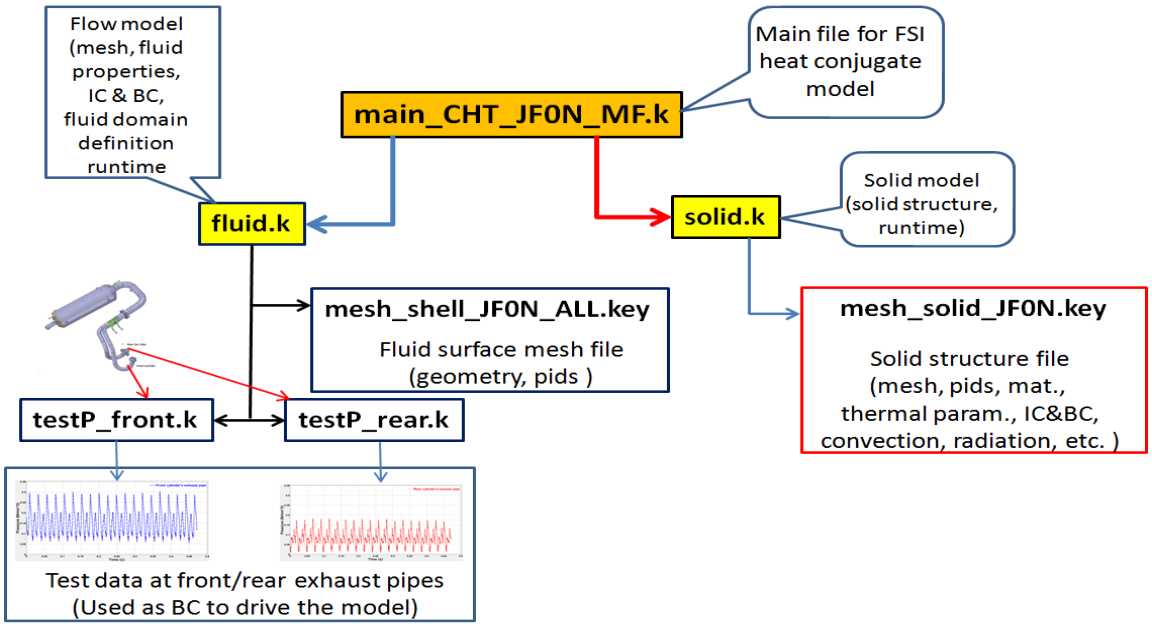

Figure 19 FSI process in conjugate heat transfer CAE model

2.2.2 Results

Figure 20 shows the correlation of CAE vs test with respect to mean pressure at the collector location shown in Figure 17. The CAE result and the measurement agree well in profile and the peak error is <2.5%. Figure 21 (a-b) show the CAE predictions of flow field and muffler surface temperature distribution.

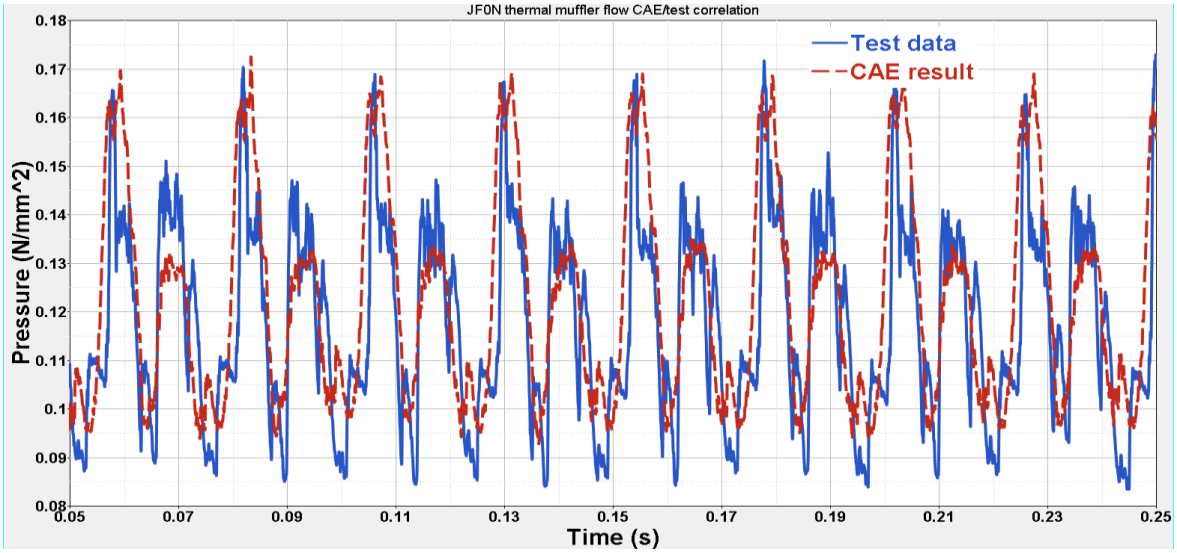

Figure 20 Correlation of CAE vs test with respect to mean pressure at collector location

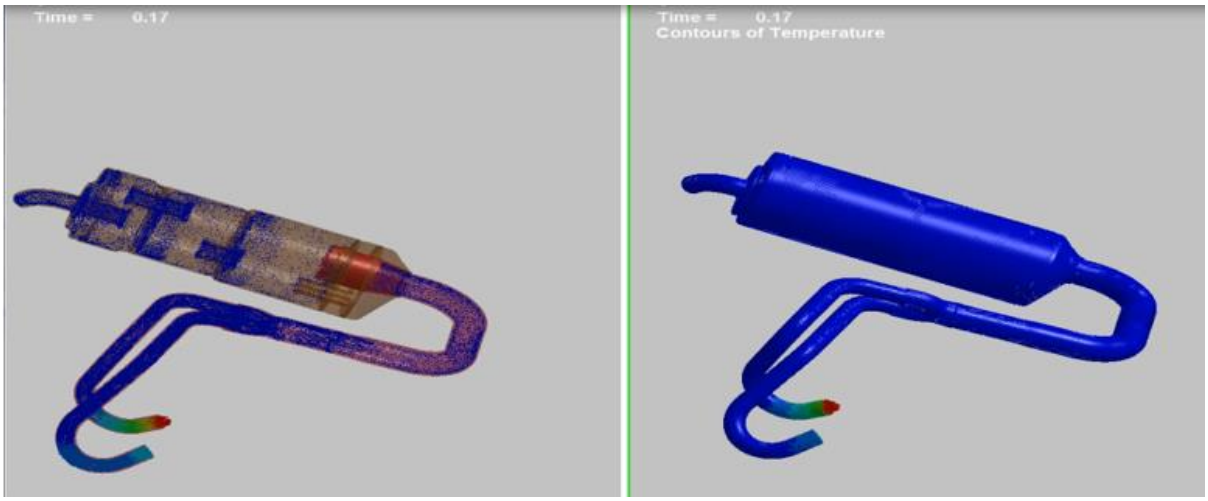

(a) Fluid field (b) Temperature contour

Figure 21 CAE conjugate heat transfer results at T=0.17 s

3. Windshield Buffeting

The objective of this work was to develop an FSI model to help judge if the window and roof of a MUV failed under aerodynamic loading from a certain wind speed.

3.1 CAE model set up

Figure 22(a-b) shows the assembly CAE meshes (ICFD fluid surface mesh and solid element mesh) of the primary steel frame (pid=10005) of an MUV with a glass window (pid=10003) and steel roof panel (pid = 10004). The initial wind speed at inlet (pid=3) is 80 mph. A non-slip condition was given to the fluid at the solid surface (pid=5) and a full-slip condition is given to the fluid at the floor (Pid=4). An atmospheric pressure of 1 mmHg is set at the outlet and lateral boundary (pid=1, 2). The steel frames were fully fixed at the joints to the underbody level as shown in Figure 22 (b).

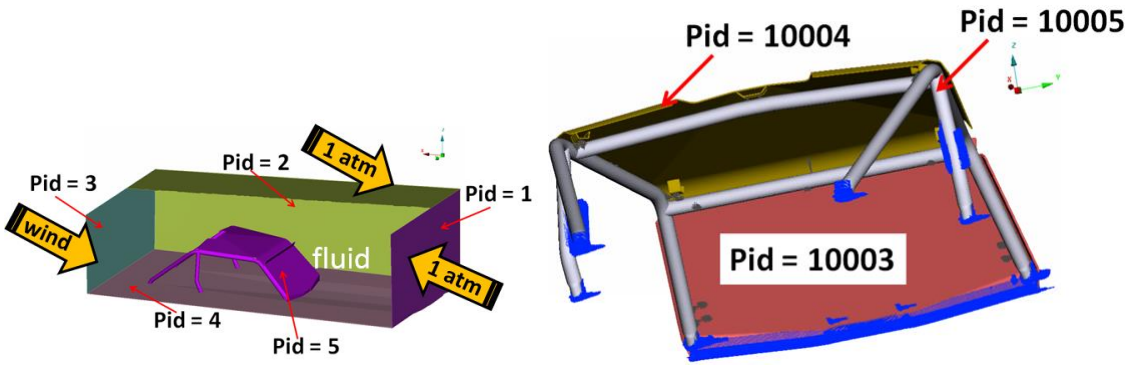

(a) ICFD fluid surface mesh (b) Solid element mesh

Figure 22 Assembled mesh for windshield buffeting in the CAE model

3.2 Results

Figure 23 (a-b) show the CAE predicted flow field and effective stress contour at the 80 mph wind speed. Figure 24 shows the displacement profile calculated at the centers of the window (point A) and roof (point B). No structural failure or detachment occurred in the model.

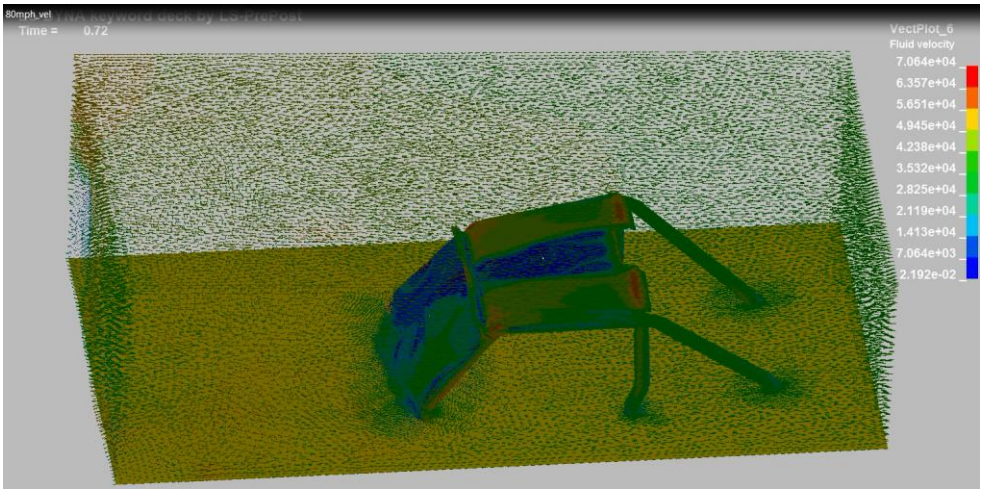

(a) Flow field

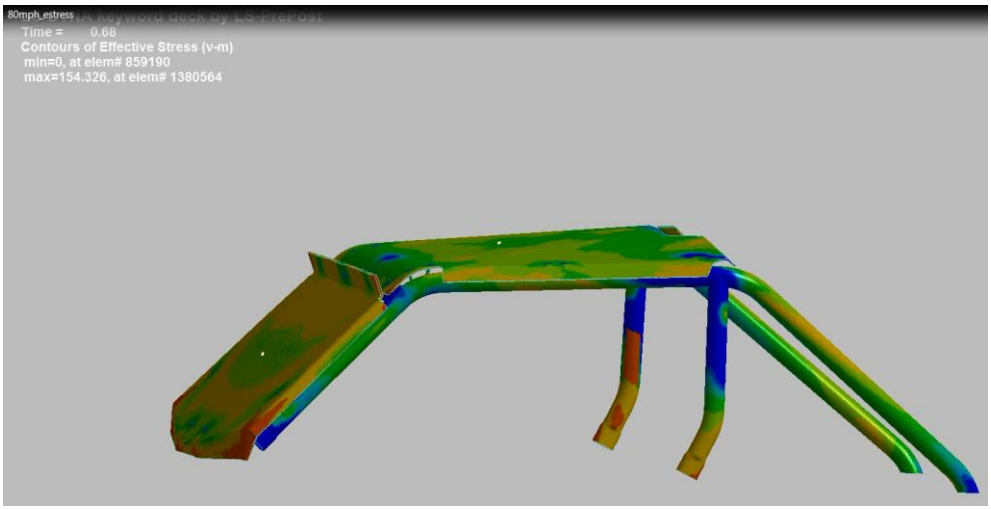

(b) Effective stress contour

Figure 23 CAE results under wind speed = 80 mph

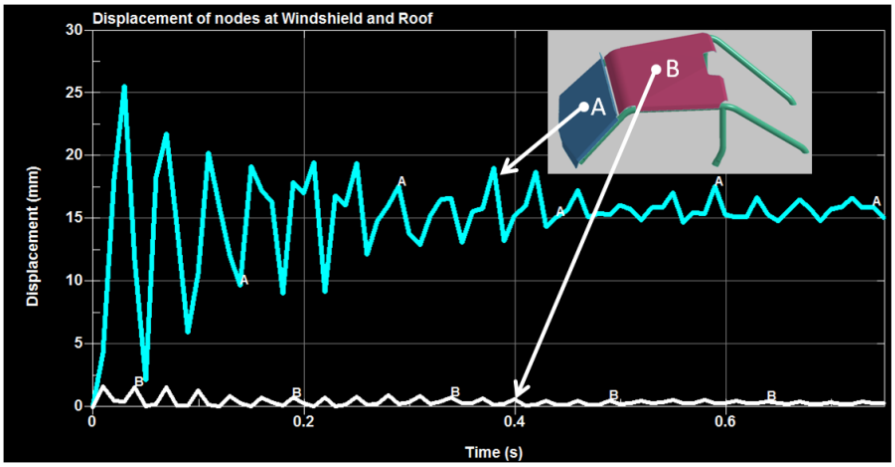

Figure 24 Displacement profile calculated at the centers of the window (point A) and roof (point B)

Conclusions

Three FSI work by using ICFD solver from LS-DYNA® were presented in this paper:

(1) Gear box oil flow driven by high spinning speed shafts with three gear box positions ($0^0, 15^0, 40^0$) and two spinning speeds (1060 and 3320 rpm) was considered. The CAE work

was to predict if oil in the gear box leaks out of the fuel hole. The CAE results completely comply with the test data.

(2) Thermal flow in muffler. The CAE results are in good agreement with the corresponding tests with respect to (i) flow rate data under constant temperature, and (ii) conjugate heat flow rate.

(3) Windshield buffeting is set up to explore if window fails by wind force. No structure failure and detachment is found.

Acknowledgements

This paper is beneficial from the valuable discussions about the test data with Tony Do and Joel Agner at Power Sports, Honda R&D Americas, Inc., OH. Glen Chamberlain and John Schirtzinger at ISD, Honda R&D Americas, Inc., gave productive support in model operation diagnostics.

References

1. *LS-DYNA® KEYWORD USER'S MANUAL VOLUME III Multi-Physics Solvers*, 10/21/16 (r:8003), LS-DYNA Dev, LIVERMORE SOFTWARE TECHNOLOGY CORPORATION (LSTC)
2. *LS-DYNA® Theory Manual*, 12/17/15 (r:7032), LS-DYNA Dev, LIVERMORE SOFTWARE TECHNOLOGY CORPORATION (LSTC)
3. Inaki Caldichoury, etc., *LS-DYNA®R7: Strong Fluid Structure Interaction (FSI) capabilities and associated meshing tools for the incompressible CFD solver (ICFD), applications and examples*, 9th European LS-DYNA Conference, Manchester, UK, 2013
4. Inaki Caldichoury, etc., *LS-DYNA®R7: Conjugate heat transfer problems and coupling between the incompressible CFD solver (ICFD) and the thermal solver, applications, results and examples*, 9th European LS-DYNA Conference, Manchester, UK, 2013
5. Inaki Caldichoury, etc., *LS-DYNA®R7: Coupled Multiphysics analysis involving Electromagnetism (EM), Incompressible CFD (ICFD) and solid mechanics thermal solver for conjugate heat transfer problem solving*, 9th European LS-DYNA Conference, Manchester, UK, 2013
6. Facundo Del Pin, etc., Advances on the Incompressible CFD Solver in *LS-DYNA®*, 11th International LS-DYNA® Users Conference, Detroit, USA, 2010
7. Bruno Boll, etc., *Coupled Simulation of the Fluid and Conjugate Heat Transfer in Press Hardening Process*, LS-DYNA Forum, Bamberg, 2014.